Automatic Library Generation for BLAS3 on GPUs

Huimin Cui*†, Lei Wang*†, Jingling Xue‡, Yang Yang*† and Xiaobing Feng*
*Institute of Computing Technology, Chinese Academy of Sciences, China
†Graduate University, Chinese Academy of Sciences, China
‡School of Computer Science and Engineering, University of New South Wales, Australia
{cuihm,wlei,yangyang,fxb}@ict.ac.cn   jingling@cse.unsw.edu.au

Abstract—**High-performance libraries, the performance-critical building blocks for high-level applications, will assume greater importance on modern processors as they become more complex and diverse. However, automatic library generators are still immature, forcing library developers to manually tune library to meet their performance objectives.**

We are developing a new script-controlled compilation framework to help domain experts reduce much of the tedious and error-prone nature of manual tuning, by enabling them to leverage their expertise and reuse past optimization experiences. We focus on demonstrating improved performance and productivity obtained through using our framework to tune BLAS3 routines on three GPU platforms: up to 5.4x speedups over the CUBLAS achieved on NVIDIA GeForce 9800, 2.8x on GTX285, and 3.4x on Fermi Tesla C2050. Our results highlight the potential benefits of exploiting domain expertise and the relations between different routines (in terms of their algorithms and data structures).

I. Introduction

Level 3 Basic Linear Algebra Subprograms (BLAS3) are performance-critical building blocks for high-level scientific applications, and highly efficient implementations of those routines enable scientists to achieve high performance at little cost. Automatically Tuned Linear Algebra Software (ATLAS) [1] is a well-known automatic BLAS3 generator, which generates efficient library implementations for platforms possessing an ANSI/ISO C compiler. Unfortunately, such tools are not yet available on the state-of-the-art many-core architectures with tens or even hundreds of cores being integrated onto a single chip, such as NVIDIA GPUs. As a result, library developers have to manually tune their applications to meet their performance objectives, which is tedious, error-prone and time-consuming [2].

A major challenge when moving to NVIDIA GPUs is how to reuse earlier tuning results. In ATLAS, the tuning results for GEMM bring benefits to a number of other BLAS3 routines. For example, the SYMM routine is implemented in a recursive way so that SYMM is split into smaller SYMM and GEMM problems. By reusing the tuning experiences for GEMM, SYMM delivers the performance close to that of GEMM (108GFLOPS for SYMM compared to 116GFLOPS for GEMM on an Intel Xeon platform). However, recursion is not efficiently supported on NVIDIA GPUs. As a result, it is not straightforward to reuse the tuning results of GEMM for other BLAS3 routines. For example, on the GTX285 platform, the performance of GEMM in CUBLAS 3.2 is 420GFLOPS while SYMM achieves only 155GFLOPS.

We are presently working on developing an automatic library generator for a number of BLAS3 routines on NVIDIA GPUs. To enable tuning experiences to be reused, our solution is to let developers focus on the differences between different library routines and specify them using the provided ADL (Adaptor Definition Language) interface. This interface enables developers to define adaptors in terms of optimization guidelines to relate a new routine with an existing one. For this purpose, we have developed an OA (Optimization Adaptor) framework based on our existing EPOD system [3]. This system provides an EPOD script interface to encapsulate existing tuning experiences into optimization schemes.

In this paper, we apply our OA framework to tune the BLAS3 library on three NVIDIA GPU platforms. Our experimental results demonstrate that our method can help library developers achieve excellent performances rapidly: up to 5.4x speedups over CUBLAS 3.2 on GeForce 9800, 2.8x for GTX285, and 3.4x for Fermi Tesla C2050.

The main contributions of this paper include:

- an adaptor definition language, which works together with EPOD scripts to relate new routines with existing ones;
- an OA framework to generate optimization schemes for new routines based the developer-provided information specified using the ADL interface; and
- experimental results showing performance speedups of up to 5.4x, 2.8x and 3.4x relative to CUBLAS 3.2 on three different NVIDIA GPU platforms.

The rest of the paper is organized as follows. Section II provides an overview of our OA framework. Section III explains the process of encapsulating existing tuning experiences into individual optimization schemes. Section IV describes how to extend existing optimization schemes into new ones for new routines. Section V presents our experimental results and analysis. Section VI discusses the related work. Section VII concludes the paper and discusses our future work.

II. The OA Framework

Figure 1 depicts our OA framework, which consists of two major components: the composer and the EPOD translator.

- **The EPOD script**. Such a script describes the optimization scheme used for a specific code region, guiding the EPOD translator to apply the optimizations specified in the script to the code region. The developers can write an EPOD script file manually in order to summarize their

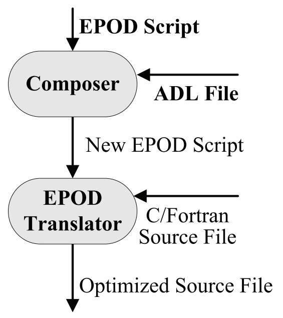

Fig. 1: An overview of our OA framework.

earlier tuning experiences. As the main contribution of this work, our OA framework enables new EPOD scripts to be automatically generated for new applications with developers' assistance.

- **The ADL file**. Such a file describes how to relate a new routine with an existing one through so-called adaptors. The ADL interface enables developers to define an *adaptor* to obtain an alternative implementation.
- **The Composer**. This module composes an existing EPOD script with the user-defined adaptors, determines how to integrate the adaptors into the script, and generates the new EPOD script(s) for the new routine.
- **The EPOD translator**. The EPOD translator is an component of our earlier EPOD framework [3], which takes EPOD scripts as input, applies the user-specified optimization schemes in the scripts to some selected code regions, and finally, generates the optimized source program (to be fed to a traditional compiler [3]).

Our OA framework will generate a set of code variants according to the composed EPOD scripts obtained. The best among the set is searched for. Optimization parameters, such as tile size, are automatically tuned with the method in [4].

In Section III, we review the EPOD translator to explain how it applies the optimization sequences specified in scripts to optimize a routine on GPUs. In Section IV, we discuss how to define an adaptor for an existing EPOD script and generate new EPOD scripts for a new routine automatically.

III. Creating an Optimization Scheme

The developers can summarize existing tuning experiences and encapsulate them into an optimization scheme in term of an EPOD script, which is passed to the EPOD translator and applied appropriately to a selected code region. In this section, we first review the EPOD translator and then explain how to express an optimization scheme using a script.

A. *The* EPOD *Translator*

Unlike traditional compilers, our translator is modularized. In traditional compilers, the optimization flow is fixed even though the user has some marginal control on the optimizations used and their phase ordering by switching on/off optimization flags. In our translator, optimization components

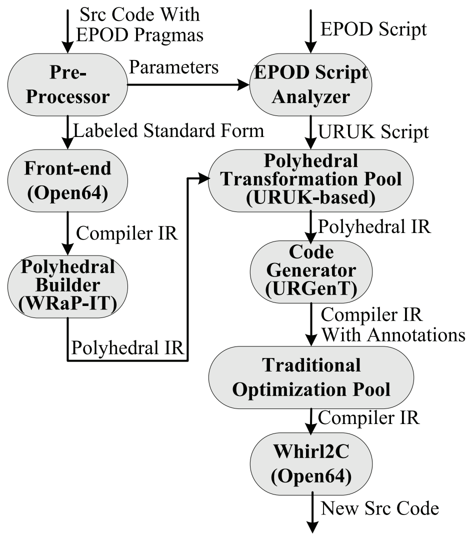

Fig. 2: An overview of EPOD translator [3].

are made available in multiple pools, where the optimizations in a pool are not pre-ordered. The user can select some components from these pools and synthesize an optimization sequence to apply to a particular code region.

In [3], we introduced a prototyping source-to-source translator with a sequential program as input. As illustrated in Figure 2, our compiler is implemented on top of the Open64 infrastructure. We included two optimization pools in our prototype. The *polyhedral transformation pool* is implemented based on URUK [5], and consists of a number of loop transformations performed in the polyhedral representation (IR). The *traditional optimization pool* is performed on Open64' compiler internal representation (IR) and implemented based on Open64. The WRaP-IT and URGenT components introduced in [5] are used for the indicated IR conversions.

As shown in Figure 2, the source code is translated into the compiler IR, which is then converted to the polyhedral IR by WRaP-IT. A URUK script is generated from the given EPOD script and the specified loop transformations are applied from the polyhedral transformation pool to the polyhedral IR. Then URGenT converts the transformed polyhedral IR back into the compiler IR, annotated with user's guidelines. Based on these annotations, the requested components in the traditional optimization pool are invoked in the user-specified order. Finally, the new compiler IR is translated back to C source code with the `whirl2c` routine in Open64. [3]

B. *The* EPOD *Script for GEMM*

In this section, we focus on the EPOD script for GEMM-NN (where "NN" means neither of the source matrices is transposed) to demonstrate the optimization components that we provide for GPUs. The scheme is derived from the work of Volkov et al [2], including the following critical steps: (1) thread grouping to distribute the iterations across thread blocks and threads in a thread block, (2) loop tiling [6] for improving

```
Labeled Source Code of GEMM-NN:
Li: for (i = 0; i < M; i++)
   Lj: for (j = 0; j < N; j++)
      Lk: for (k = 0; k < K; k++)
           C[i][j] += A[i][k] * B[k][j];
```

```
EPOD Script for GEMM-NN:
 (Lii, Ljj) = thread_grouping((Li, Lj));
 (Liii, Ljjj, Lkkk) = loop_tiling(Lii, Ljj, Lk);
 loop_unroll(Ljjj, Lkkk);
 SM_alloc(B, Transpose);
 reg_alloc(C);
```

Fig. 3: The EPOD script for GEMM-NN on GPUs.

locality, (3) loop unrolling, (4) allocating the source sub-matrices in shared memory, and (5) allocating the destination sub-matrices in registers. Each of these steps is mapped to an optimization component in our two optimization pools.

Figure 3 presents the EPOD script for GEMM-NN. The matrices are assumed to be stored in column major to be consistent with BLAS3. Note that the loops in a loop nest are labeled (e.g., `Li`, `Lj`, and `Lk`) so that they can be identified by various loop transformations. In Figure 3, the two components, `loop_tiling` and `loop_unroll`, are intuitive but the other three are more complex and discussed below.

- **thread_grouping**. This optimization aims to expose two-level parallelism, by distributing loop iterations across the thread blocks and threads within a thread block. Our polyhedral-based implementation is similar to the one presented by Baskaran et al in [7]. Loop tiling is used at the first step to generate multi-level parallel tiled code. Furthermore, thread distribution is used to replace the loop indices for parallel iterations into block and thread index, `blockIdx` and `threadIdx`, in CUDA. After thread_grouping has been applied, the workload distribution of the routine is shown in Figure 4.

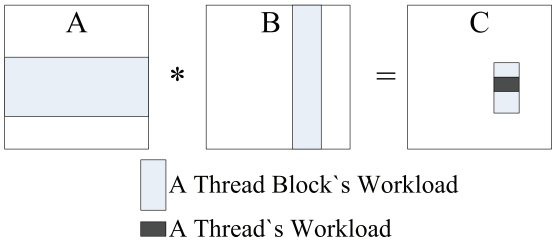

Fig. 4: Workload Distribution of GEMM-NN.

- **SM_alloc**. This optimization explicitly specifies that some variables are allocated in shared memory. By default, all data are located in global memory. This optimization invocation creates a copy of a specified object in shared memory in a specified allocation mode. Presently, three allocation modes are:
  `NoChange` $(dest = src)$
  `Transpose` $(dest = src^T)$
  `Symmetry` $(dest = src + src^T - diag(src))$

  For the `SM_alloc` optimization invoked in Figure 3, `Transpose` is used to yield stride-1 accesses to shared memory in the inner loop of GEMM-NN [2].
  Note that library developers are only required to specify which objects are placed in shared memory and how they are placed in terms of allocation modes. Our framework will automatically determine the data mapping induced and generate the data movement statements required. In addition, padding is done automatically to reduce bank conflicts. For example, a two-dimensional array of size (16, 16) will be padded to (16, 17) for memory efficiency.
- **Reg_alloc**. This optimization explicitly maps some variables into registers. As in `SM_alloc`, our EPOD translator automatically determines the data mapping induced and generates the data movement statements required.

For the other optimizations not used for GEMM-NN but provided for other routines in BLAS3 in our optimization pools, we will discuss them in Section IV when they are invoked.

IV. Extend to New Optimization Scheme

We discuss how to define four adaptors used in BLAS3, Adaptor_Transpose, Adaptor_Symmetry, Adaptor_Triangular and Adaptor_Solver. We describe how our composer works by showing how the optimization scheme used in GEMM-NN is extended to more routines. As before, a matrix is assumed to be stored in column major to be consistent with BLAS3.

A. The Adaptor Definition Language (ADL)

An *adaptor* is defined to adapt an optimization scheme for a routine involving matrices to others with some matrix variations, focusing on the matrices themselves instead of the operations applied to them. The ADL is provided for developers to describe an adaptor in terms of compiler optimizations.

```
adaptor_name(object):
   | optimization components invocation sequence 1
     {cond(condition 1)}
   | optimization components invocation sequence 2
     {cond(condition 2)}
   | ...
```

With this syntax, the alternative implementations of an adaptor can be defined so that multiple optimization schemes will be generated, enabling the best one to be selected by a search. Furthermore, developers can specify optional conditions for each implementation so that multiple-versioned code can be generated (to be discussed using Adaptor_Triangular).

1) Adaptor_Transpose: This adaptor is defined as follows:

```
Adaptor_Transpose(X):
   | GM_map(X, Transpose);
   | SM_alloc(X, Transpose);
```

which specifies its three alternative implementations: (1) the empty rule keeps `X` unchanged in global memory and the transposition is not applied to the matrix until accessed, (2) the `GM_map` rule transposes `X` in global memory, which means the transposition is applied before the matrix is used (implying that the optimization scheme of GEMM-NN can be applied), and (3) the `SM_alloc` rule specifies that the transposition is applied to sub-matrices, if possible, in which case, our composer will determine the size of shared memory allocated.

Below we examine `GM_map`, which is implemented based on the polyhedral IR, including the following steps:

- Step 1. Generate statements for memory allocation and data mapping. In the case of the `Transpose` mode, the corresponding statements are:

```
for (i = 0; i < M; i++)
    for (j = 0; j < N; j++)
        NewX[i][j] = X[j][i];
```

- Step 2. Distribute the above statements across the CUDA thread blocks and threads within a thread block, using the method similar as the one used for `thread_grouping`.
- Step 3. Modify the subscript in the polyhedral IR [5] to replace the reference of `X[i][j]` with `NewX[j][i]`.

In our OA framework, `GM_map` is valid only when it is the first optimization in an optimization sequence.

2) Adaptor_Symmetry: This is designed for symmetric matrices. Figure 5 shows a symmetric matrix with only its left lower triangular area stored. For such a matrix, the accesses can be divided into a *real area* and a *shadow area*. The shadow area is not stored explicitly but derived from the real area.

The following code segment shows a typical access pattern to a symmetric matrix A:

```
for (i = 0; i < M; i++)
{
    for (k = 0; k < i; k++)
    {
        ...A[i][k]; //for real area
        ...A[i][k]; //for shadow area
    }
    ...A[i][i]; //for diagonal elements
}
```

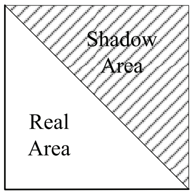

Fig. 5: Computation split for SYMM on GPUs.

In the innermost loop of the above code, two accesses to A[i][k] are included, with the first to the real area and the second to the shadow area. As a result, A is accessed in a mixed mode (row major for the first part and column major for the second part). However, in scientific computations, a matrix is preferred to be efficiently accessed in either row or column major (but not both). We use Adaptor_Symmetry to re-format such a loop nest to remove the mixed-mode accesses:

```
Adaptor_Symmetry(X):
    | GM_map(X, Symmetry);
      format_iteration(X, Symmetry);
    | format_iteration(X, Symmetry);
      SM_alloc(X, Symmetry);
```

Like Adaptor_Transpose, this adaptor supports three alternative implementations. The empty rule keeps `X` unchanged. The second rule applies first `GM_map(X, Symmetry)` to obtain a matrix containing both the real and shadow areas with the computation of $X + X^T - Diag(X)$ and then `format_iteration`, which is composed of loop fission and fusion, to the new matrix. Both components work together to transform the above loop nest into the standard GEMM-NN. Therefore, the optimization scheme of GEMM-NN can then be applied. We will discuss `format_iteration` in detail below. The third rule invokes `format_iteration` but loop fusion will fail (as discussed below). Then `SM_alloc` seeks for appropriate sub-matrices to be allocated in shared memory.

The `GM_map` and `SM_alloc` components are discussed in earlier sections. Below we discuss `format_iteration`, focusing on the second rule for Adaptor_Symmetry. In this second rule, `GM_map` is applied before `format_iteration` is invoked. As a result, the above-mentioned loop nest has been turned into:

```
for (i = 0; i < M; i++)
{
    for (k = 0; k < i; k++)
    {
        ...NewA[i][k];   //for real area
        ...NewA[k][i];   //for shadow area
    }
    ...NewA[i][i];   //for diagonal elements
}
```

There are three steps involved in `format_iteration`:

- Step 1. Loop fission is applied to the accesses of `X` so that the loop nest is split into three with each containing accesses to `X`'s three disjoint areas, called real-area-access, shadow-area-access, and diag-area-access, respectively:

```
for (i = 0; i < M; i++)
{
    for (k = 0; k < i; k++)
        ...NewA[i][k];   //for real area
    for (k = 0; k < i; k++)
        ...NewA[k][i];   //for shadow area
    ...NewA[i][i]; //for diagonal elements
}
```

- Step 2. After Step 1, the loop nest for real-area-access accesses `X` in row major and the loop nest for shadow-area-access accesses `X` in column major. When the column major order is detected, loop interchange is applied to change it into the row major order:

```
for (i = 0; i < M; i++)
{
    for (k = 0; k < i; k++)
        ...NewA[i][k]; //for real area
    for (k = i+1; k < K; k++)
        ...NewA[i][k]; //for shadow area
    ...NewA[i][i]; //for diagonal elements
}
```

- Step 3. Loop fusion is applied if possible. If loop interchange was applied earlier, there may be an opportunity to fuse all loop nests to obtain the standard GEMM-NN. The code shown in Step 2 can be fused into:

```
for (i = 0; i < M; i++)
    for (k = 0; k < K; k++)
        ...NewA[i][k];
```

In summary, the basic idea behind `format_iteration` is to apply loop fission and fusion whenever possible. Therefore, for the third rule of Adaptor_Symmetry, the loop nests cannot be fused after loop fission so that `format_iteration` degenerates into a simple loop fission. The unfusable code after loop fission is:

```
for (i = 0; i < M; i++)
{
    for (k = 0; k < i; k++)
        ...A[i][k];   //for real area
    for (k = 0; k < i; k++)
        ...A[i][k];   //for shadow area
    ...A[i][i]; //for diagonal elements
}
```

3) Adaptor_Triangular: This adaptor applies to a triangular matrix. Unlike a symmetric matrix, which can derive its shadow area from its real area, a triangular matrix induces only accesses to the real area. Its typical access pattern is:

```
for (i = 0; i < M; i++)
{
    for (k = 0; k <= i; k++)
    {
        ...A[i][k];
    }
}
```

The triangular iteration space would cause the threads in a thread block to exhibit different loop bounds (called *un-uniform loop bounds*), thereby decreasing performance. Our adaptor implementation addresses on this performance issue in two ways, loop peeling and padding, as illustrated in Figure 6. The first separates the triangular areas from rectangular ones to reduce the effects of un-uniform loop bounds on performance. The second pads the triangular iteration spaces into rectangular ones to eliminate un-uniform loop bounds completely. Note that the blank areas must be cleared as 0's. Otherwise the padded iterations would generate unpredictable results.

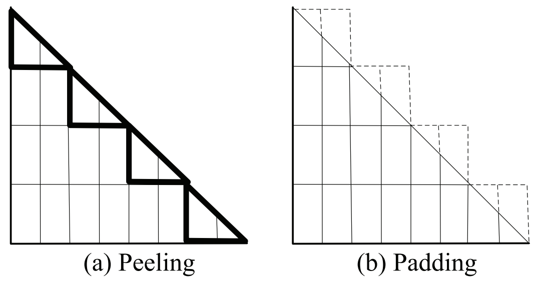

Fig. 6: Peeling and padding for a triangular matrix.

Therefore, this adaptor is implemented as follows:

Adaptor_Triangular(X):
  | *peel_triangular(X);*
  | *padding_triangular(X);* {*cond(blank(X).zero = true)*}

There are two components invoked in the adaptor implementation: `peel_triangular` and `padding_triangular`. They work with the following steps:

- Step 1. Expose the X-access loop nest and detect for the trapezoid areas. Note that for a triangular area, the detection will fail before loop tiling is applied.
- Step 2. If a trapezoid area is detected, `peel_triangular` peels the triangular area off the rectangular ones, while `padding_triangular` pads the triangular area into another rectangular one.

In the third rule of Adaptor_Triangular, we require that `blank(X).zero = true`. This will lead the OA framework to generate multiple-version code as follows:

```
int blank_zero = check_blank_zero(X);
if (blank_zero)
{
    //code for padded triangular area.
}
else
{
    //code without padding.
}
```

4) Adaptor_Solver: This adaptor, which comes from the TRSM routine in BLAS3, updates a matrix on-the-fly:

```
for (i = 0; i < M; i++)
    for (j = 0; j < N; j++)
        for (k = 0; k <= i; k++)
            B[i][j] = ...B[k][j];
```

The access pattern is similar to that in TRMM with the difference that the dependence from `B[i][j]` to `B[i+1][j]` prevents the sub-matrices along the `i` dimension from being computed in parallel. This problem can be handled by `thread_grouping`. Therefore, the thread grouping returns a different workload distribution from GEMM-NN with the adjusted work load for a thread block as shown Figure 7.

As shown in Figure 7, the workload of each thread block is separated into two parts. Let us take B2 as an example. `B2-A20*B0-A21*B1` can be simultaneously executed by the threads in a thread block, but the final step `B2=TRSM(A22,B2)` has to be sequentially executed by only one thread. Therefore, the adaptor is defined as follows:

```
Adaptor_Solver(X):
  | peel_triangular(X);
    binding_triangular(X, 0);
```

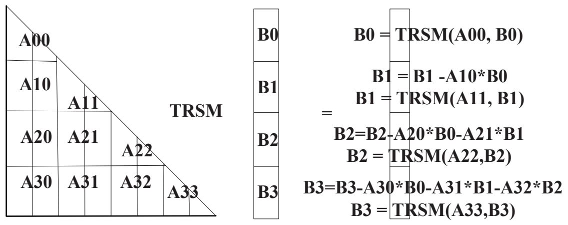

Fig. 7: Workload Distribution for Adaptor_Solver.

The `binding_triangular` component seeks for a triangular area and forces it to be executed in sequential mode. Therefore, the corresponding code is bounded to an individual thread in a thread block. The implementation is flexible enclosing the code region for the triangular area with a condition of $threadIdx.x == 0 \&\& threadIdx.y == 0$.

B. The Composer

The composer takes an existing EPOD script and an adaptor as input, composes the referenced optimization components together, and derives one (or more) new EPOD scripts for each adaptor implementation. There are five major components: splitter, mixer, filter, allocator and generator.

The major workflow is shown in Figure 8. The splitter splits an optimization sequence into a polyhedral part and a traditional part, which are fed to the mixer and allocator, respectively. The mixer mixes the two polyhedral transformation sequences together and generates multiple resulting sequences, with illegal sequences filtered out by the filter. Meanwhile, the traditional transformations are analyzed and the memory allocation schemes (traditional transformations) are determined by the allocator. Finally, the legal polyhedral transformations and memory allocation schemes are merged together and new EPOD scripts are generated.

The splitter and generator are straightforwardly implemented. Below we discuss the mixer, filter and allocation in detail.

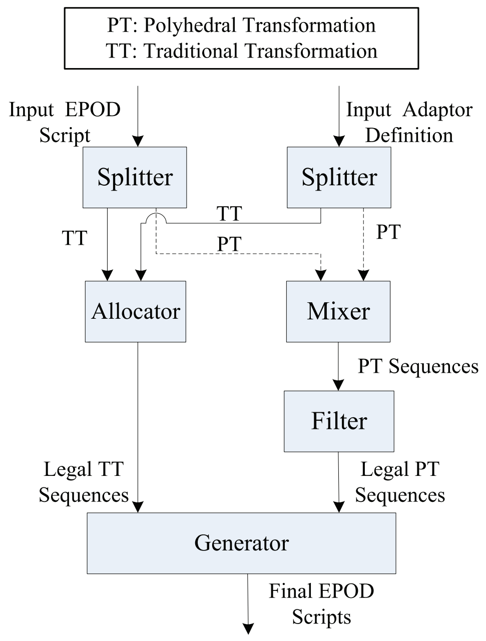

Fig. 8: The Composer Framework.

1) Mixer: This component mixes two polyhedral transformation sequences. As shown in Figure 9, A and B are mixed together. The mixer interleaves components from A and B together. Meanwhile, the order of components from the same sequence is strictly kept. Then the mixer checks location constraints for each component and generates the mixed transformation sequence if the constraints are satisfied. For example, `GM_map` should be fixed as the first in a sequence if it appears. Therefore, the mixer does not generate any sequences violating this condition.

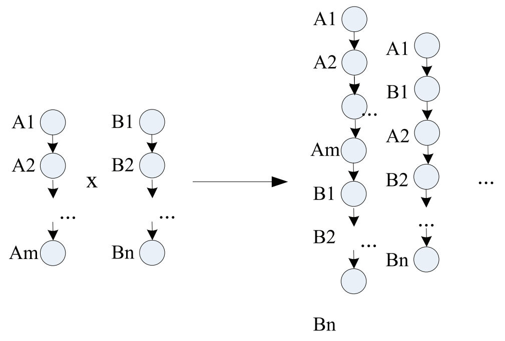

Fig. 9: The Mixing Process.

2) Filter: This component tries every transformation sequence generated by the mixer and applies the transformation component by component. If a specific constraint for some component is not satisfied, then the corresponding component is omitted. For example, after Adaptor_Triangular and the EPOD script of GEMM-NN have been mixed, the following sequences will be the input of the filter:

1) thread_grouping, loop_tiling, loop_unroll
2) peel_triangular, thread_grouping, loop_tiling, loop_unroll
3) thread_grouping, peel_triangular, loop_tiling, loop_unroll
4) thread_grouping, loop_tiling, peel_triangular, loop_unroll
5) thread_grouping, loop_tiling, loop_unroll, peel_triangular
6) padding_triangular, thread_grouping, loop_tiling, loop_unroll
7) thread_grouping, padding_triangular, loop_tiling, loop_unroll
8) thread_grouping, loop_tiling, padding_triangular, loop_unroll
9) thread_grouping, loop_tiling, loop_unroll, padding_triangular

Sequences 1, 3, 4, 7, 8 are successfully applied and thus added to a sequence set, denoted *semi-output*. For Sequences 2 and 6, peel_triangular fails because it cannot detect a trapezoid area; they degenerate into Sequence 1. For Sequences 5 and 9, loop_unroll fails due to the existence of the non-rectangular areas; they degenerate into the following two sequences, which are added into *semi-output*:

1) thread_grouping, loop_tiling, peel_triangular
2) thread_grouping, loop_tiling, padding_triangular

In summary, the *semi-output* of the filter includes seven sequences. These sequences are checked to ensure that data dependences are satisfied with the PolyDeps tool [8]. Illegal ones are removed and the legal ones generated.

3) Allocator: The allocator integrates the memory allocation invocations in the given EPOD script and the adaptor and analyzes and determines the final memory allocation scheme, including which memory hierarchy a matrix should reside in and the granularity of the memory allocation. Note that GM_map is not considered because it is a polyhedral-based transformation and must be applied at the first step.

Consider the matrix multiplication of the form $C = \alpha A^T * B + \beta C$. The adaptor defines one rule that declares A to be allocated in shared memory, which does not conflict with those in the EPOD script, so that the declaration is kept.

When we turn to another variation of GEMM, $C = \alpha A * B^T + \beta C$, the adaptor still declares B to be allocated in shared memory in the Transpose mode. Meanwhile, the EPOD script also declares B in the same way. In this case, the allocator integrates both together and generates one declaration of SM_alloc(B, NoChange).

The memory allocation and the corresponding statements are processed when SM_alloc is executed, using the method in [9]. This will not be discussed any further in the paper.

V. Performance Evaluation and Analysis

We evaluate our work on three GPU platforms: GeForce 9800, GTX285 and Fermi Tesla C2050. In this paper, we focus on single-precision floating point computations.

- The GeForce 9800 platform consists of 16 streaming multiprocessors (SMs), each containing 8 streaming processors (SPs). Each SM has 8192 registers and a 16KB local scratchpad memory shared by all simultaneously active threads in the SM. The peak performance is 429GFLOPS.
- The GTX285 platform consists of 30 SMs, each containing 8 SPs. Each SM has 16384 registers and a 16KB local scratchpad memory shared by all simultaneously active threads in the SM. The peak performance is 709GFLOPS.
- The Fermi Tesla C2050 platform consists of 14 SMs, each containing 32 SPs. Each SM has 32768 registers and a 48KB local scratchpad memory (configured to be) shared by all simultaneously active threads in the SM. The peak performance is over a Tera FLOPS.

The original BLAS3 source programs are first transformed by our OA framework. Then the transformed source code is compiled by nvcc with the -O2 optimization flag.

A. Results

Our main results can be summarized as follows:

- Our method can achieve better performances for 24 variants of BLAS3 routines than those provided in CUBLAS 3.2 with up to 5.4x speedups being achieved;
- Our method has successfully narrowed the performance gaps between matrix-multiplication variants and the GEMM-NN routine, showing the benefits of optimizing libraries by exploiting existing tuning results; and
- Our method shows that it can yield stable performances for BLAS3 routines for varying problem sizes.

As discussed earlier, our OA framework will generate multiple alternative EPOD scripts for a given routine with the best performer being selected by a search.

Figure 10 – 12 show the performance speedups for the 24 variants of BLAS3 routines on the three platforms compared with CUBLAS 3.2. These variants are identified by different postfixes. For example, TRSM-LL-N is a variant of TRSM such that LL stands for "**L**eft **L**ower triangular" and N stands for "**N**o transposed." The problem size is fixed as 4096. We also compare our method with MAGMA v0.2 [10] on GTX285 using the GEMM and TRSM variants, as shown in Figure 11 (SYMM and TRMM variants are not compared due to their absence in MAGMA library). Our method achieves better performances than MAGMA v0.2. The MAGMA performances on the Geforce and Fermi platforms are not presented because MAGMA performs no better than CUBLAS on Geforce and the MAGMA library on Fermi has included only the GEMM routine.

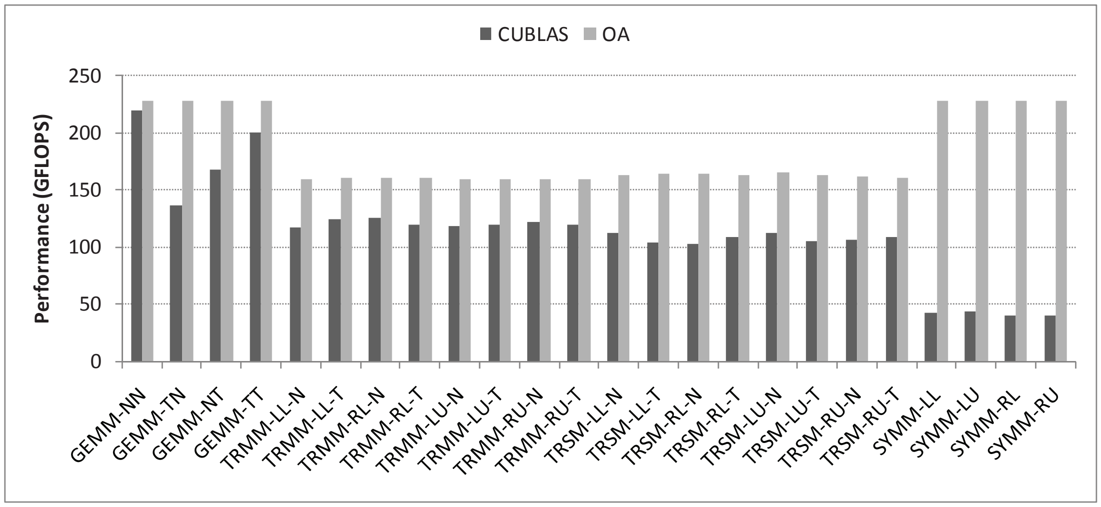

Fig. 10: Performance of BLAS3 on GeForce 9800.

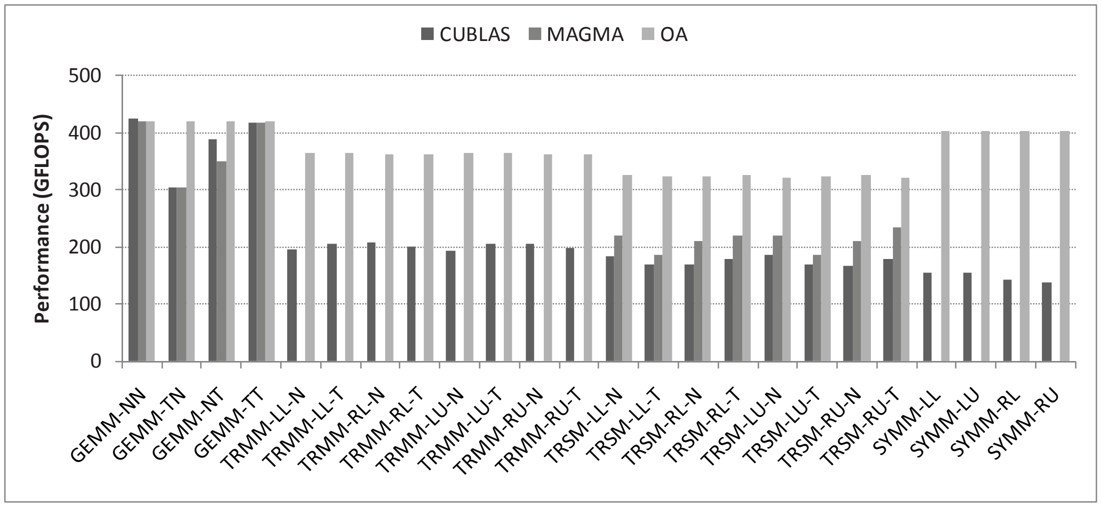

Fig. 11: Performance of BLAS3 on GTX 285.

1) Speedups Over CUBLAS: Our experimental results show that up to 2.8x speedups over the CUBLAS library are achieved on GTX 285, 5.4x on GeForce 9800, and 3.4x on Fermi Tesla C2050. Specifically, the performance of SYMM routines increases from 155GFLOPS to 403GFLOPS on GTX 285, and from 42GFLOPS to 225GFLOPS on GeForce 9800.

The performance comparison for SYMM is the most glaring, so we focus on it to compare the profiles of our OA generated code with CUBLAS 3.2 (ssymm_main_hw_lo_left_fulltile routine) for the problem size 4096. Table I shows some profile data collected with `cuda_profile` on GeForce 9800.

The profile results show that two issues contribute to the performance speedups of OA over CUBLAS: (1) the number of instructions executed, which is halved by OA, and (2) the number of *gld_incoherent* (non-coalesced global memory) loads executed, which is completely removed by OA. Our method has successfully coalesced the global memory addresses simultaneously accessed by each thread of a half-warp into a single contiguous aligned memory access.

TABLE I: Profiles of SYMM for OA and CUBLAS 3.2 on GeForce 9800. Here, *gld_incoherent* stands for non-coalesced global memory loads, *gld_coherent* for coalesced global memory loads, *gst_incoherent* for non-coalesced global memory stores, *gst_coherent* for coalesced global memory stores, and *instructions* for dynamic number of instructions.

Events	**CUBLAS**	OA
gld_incoherent	*134M*	*0*
gld_coherent	25M	42M
gst_incoherent	0	0
gst_coherent	0.52M	1.04M
instructions	*340M*	*167M*

For SYMM on GTX285, the performance gap between OA and CUBLAS is smaller, because the non-coalesced memory

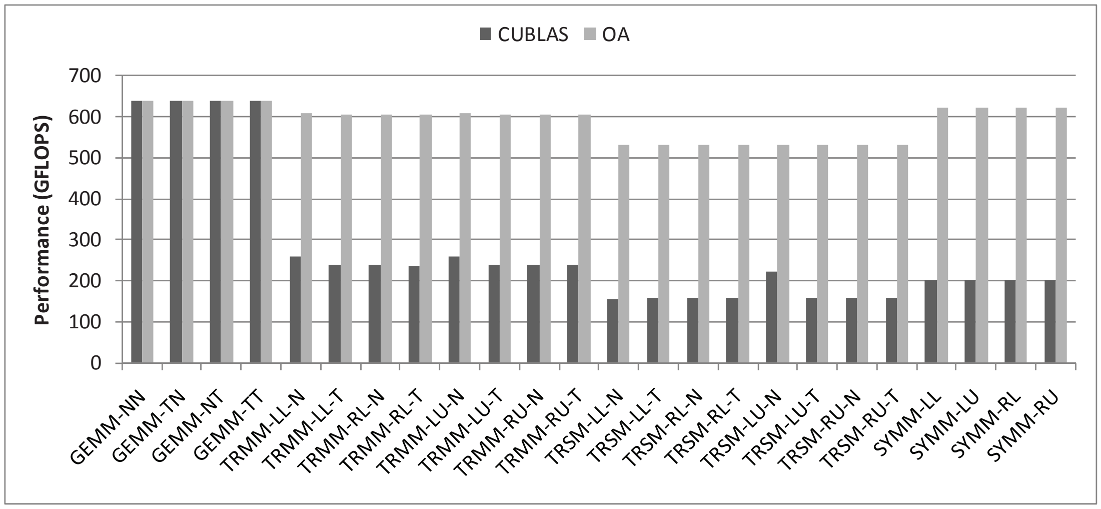

Fig. 12: Performance of BLAS3 on Fermi Tesla C2050.

read problem in CUBLAS did not show up. The performance improvement made by OA mainly comes from the reduced instruction count, as shown in Table II.

TABLE II: Profiles of SYMM for OA and CUBLAS 3.2 on GTX285.

Events	**CUBLAS**	OA
gld_incoherent	*0*	*0*
gld_coherent	127M	33M
gst_incoherent	0	0
gst_coherent	0.42M	0.84M
instructions	*181M*	*88M*

On the Fermi Tesla C2050 platform, the profiler cannot provide the memory coalescing statistics. So we collected the global/local memory access events and executed instructions. As shown in Table III, the performance improvement made by OA mainly comes from reductions on both the number of instructions and the number of global loads executed.

TABLE III: Profiles of SYMM for OA and CUBLAS 3.2 on Fermi Tesla C2050. Here, *gld_request* stands for the number of global loads per warp in a SM, *gst_request* for the number of global stores per warp in a SM, *local_read* for the number of local loads per warp in a SM, *local_store* for the number of local stores per warp in a SM, and *inst_executed* for the number of instructions executed.

Events	**CUBLAS**	OA
gld_request	*14.53M*	*0.08M*
gst_request	0.05M	0.05M
local_read	0	0.87M
local_store	0M	0.18M
inst_executed	*805M*	*336M*

2) Narrowing the Performance Gap: Furthermore, Figures 10, 11, and 12 show that the performances of the 24 BLAS3 routine variants achieved by our OA method are comparable to that of GEMM-NN. In contrast, the CUBLAS performances fluctuate drastically across these routines. For example, when moving from GEMM-NN to SYMM-LL on GTX285, the performance drops from 420GFLOPS to 155GFLOPS. Our method has succeeded in narrowing such performance gap.

3) Achieving the Scalable Performance: Figure 13 presents our performance results with the problem sizes varying from 512 to 4096 on GeForce 9800. Similar results can be observed on GTX 285 and Fermi Tesla C2050. Our experimental results show that our OA framework can achieve stable performances for BLAS3 routines when the problem size varies.

B. Best-Performing EPOD *Scripts*

In our implementation, our OA framework automatically generates multiple EPOD scripts for each routine, and search ing is used to select the best-performing one. Figure 14 lists the best-performing scripts for some routines.

VI. Related Work

In order to assist library developers in managing programming complexity, auto-tuning was developed by some library writers, including ATLAS [1], FFTW [11]and SPIRAL [12]. These systems perform a systematic search over a collection of automatically generated code variants. On the state-of-the-art architecture platforms, the auto-tuning technology has been applied to some specific applications, such as sparse matrix-vector multiply [13], stencil computations [14], and dense linear algebra [2]. There are some related efforts on integrating compiler model-based methods into an auto-tuner in order to automatically generate and search a set of alternative implementations [15], [16]. These efforts focus on pre-determined code variant selection and parameter tuning for a specific

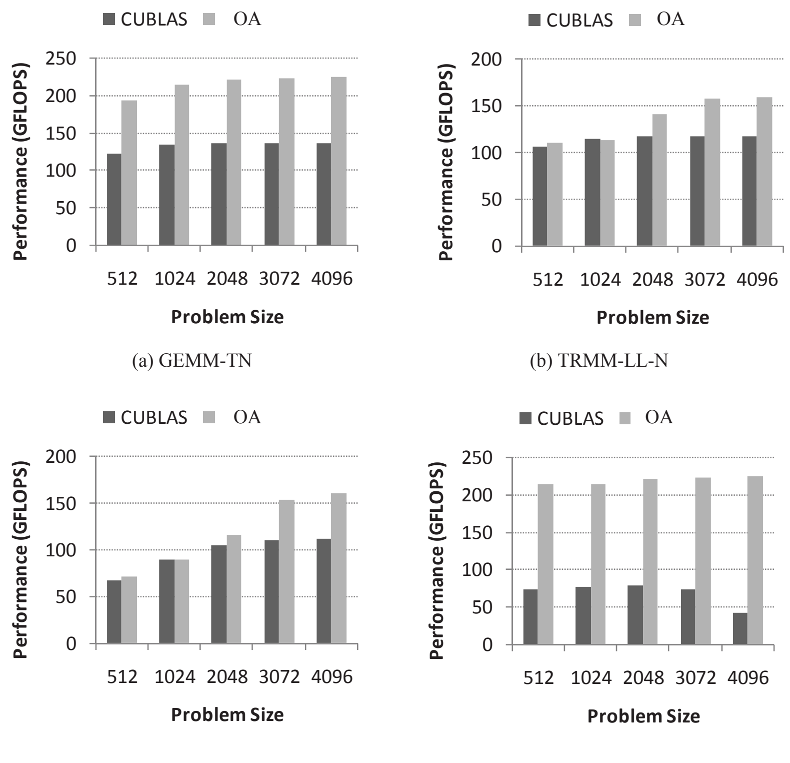

(a) GEMM-TN (b) TRMM-LL-N

(c) TRSM-LL-N (d) SYMM-LL

Fig. 13: Performance results with varying problem sizes on GeForce 9800.

application. In contrast, our work provides a general-purpose framework to allow library developers to tune an optimization scheme in a larger search space in a more flexible manner.

Iterative compilation is another research area to bridge the gap between performance obtained by automatic and manual optimizations [17], [18], [19], [20], which is an application-independent technology and typically hunts for the best optimization sequence from the search space involving optimization flags, parameters and phase ordering. Some researchers [21], [22] show that iterative compilation can achieve competitive performance to hand-tuned code for specific applications. There have been some research efforts on reducing the search space [23], [24], [25]. On modern processors with the state-of-the-art hardware features such as GPUs, Liu et al [26] present a G-ADAPT framework for performing an iterative search across a set of compiler parameter values.

To support active involvement of domain experts, researchers are experimenting with collective optimization [27], [28], [29] in the self-optimizing compiler framework, MILEPOST GCC. The idea is to collect performance information in a central database shared across different users and relies on machine learning to compare semantic features and select good optimization passes [29]. Rather than exploiting similarity between applications, this work enables developers to explicitly only describe the difference between routines.

The use of scripting language for optimization has been presented in [30], [4], [31], [5], and proven to be a flexible way to apply some optimizations for specific code regions. Therefore, we have extended this method to provide high-level optimization components as the underlying component.

VII. Conclusions

We have presented a script-controlled compilation framework, OA, for accelerating library development on GPUs and introduced the performance tuning process for BLAS3 routines. Our experimental results show that OA can be used to improve the productivity of library development while promising to deliver good performances. Specifically, on NVIDIA GPUs, up to 5.4x speedups over CUBLAS 3.2 are achieved on GeForce 9800, 2.8x on GTX285 and 3.4x on Fermi Tesla C2050. These results demonstrate the benefits in performance tuning by reusing existing optimization experiences.

In future, we will extend our method to more routines and multi-GPUs, which provide more opportunities and challenges for automatic library generators.

VIII. Acknowledgements

We would like to thank all anonymous reviewers for their comments and suggestions.

This research is supported in part by Chinese National Basic Research Grants 2011CB302500 and 2011CB302504, an Innovation Research Group of NSFC 60921002, a National Science and Technology Major Project of China 2009ZX01036-001-002, National Natural Science Foundations of China

GEMM-TN
```
Source code:
Li: for (i = 0; i < M; i++)
    Lj: for (j = 0; j < N; j++)
        Lk: for (k = 0; k < K; k++)
               C[i][j] += A[k][i]  * B[k][j]

EPOD Script:
    GM_map(A, Transpose);
    (Lii, Ljj) = thread_grouping(Li, Lj);
    (Liii, Ljjj, Lkkk) =
               loop_tiling(Lii, Ljj, Lkk);
    loop_unroll(Ljjj, Lkkk);
    SM_alloc(B, Transpose);
    reg_alloc(C);
```

SYMM-LN
```
Source Code:
Li: for (i = 0; i < M; i++)
    Lj: for (j = 0; j < N; j++)
    {
       Lk: for (k = 0; k < i; k++)
           {
               C[i][j] += A[i][k] * B[k][j];
               C[k][j] += A[i][k] * B[i][j];
           }
       Ld: C[i][j] += A[i][i] * B[i][j]
    }

EPOD Script:
    GM_map(A, Symmetry);
    format_iteration(A, Symmetry);
    (Lii, Ljj) = thread_grouping(Li, Lj);
    (Liii, Ljjj, Lkkk) =
               loop_tiling(Lii, Ljj, Lkk);
    loop_unroll(Ljjj, Lkkk);
    SM_alloc(B, Transpose);
    reg_alloc(C);
```

TRMM-LL-N
```
Source Code:
Li: for (i = 0; i < M; i++)
    Lj: for (j = 0; j < N; j++)
        Lk: for (k = 0; k <= i; k++)
               C[i][j] += A[i][k] * B[k][j]

EPOD Script:
    (Lii, Ljj) = thread_grouping(Li, Lj);
    (Liii, Ljjj, Lkkk) =
               loop_tiling(Lii, Ljj, Lkk);
    padding_triangular(A);
    loop_unroll(Ljjj, Lkkk);
    SM_alloc(B, Transpose);
    reg_alloc(C);
```

TRSM-LL-N
```
Source Code:
Li: for (i = 0; i < M; i++)
    Lj: for (j = 0; j < N; j++)
        Lk: for (k = 0; k < i; k++)
               B[i][j] -= A[i][k] * B[k][j]

EPOD Script:
    (Lii, Ljj) = thread_grouping(Li, Lj);
    (Liii, Ljjj, Lkkk) =
               loop_tiling(Lii, Ljj, Lkk);
    binding_triangular(A, 0);
    loop_unroll(Ljjj, Lkkk);
    SM_alloc(B, Transpose);
    reg_alloc(C);
```

Fig. 14: Best-performing EPOD Scripts for some BLAS3 Routines.

(60970024 and 60633040), a Beijing Natural Science Foundation 4092044, and an Australian Research Council (ARC) Grant DP0987236.

REFERENCES

[1] R. C. Whaley, A. Petitet, and J. Dongarra, "Automated empirical optimizations of software and the atlas project," in *Parallel Computing*, 2001.

[2] V. Volkov and J. Demmel, "Benchmarking gpus to tune dense linear algebra," in *Proc. Supercomputing*, 2008.

[3] H. Cui, J. Xue, L. Wang, Y. Yang, X. Feng, and D. Fan, "Extendable pattern-oriented directives," in *CGO*, 2011.

[4] A. Tiwari, C. Chen, J. Chame, M. Hall, and J. K. Hollingsworth, "A scalable auto-tuning framework for compiler optimization," in *IPDPS*, 2009.

[5] S. Girbal, N. Vasilache, C. Bastoul, A. Cohen, D. Parello, M. Sigler, and O. Temam, "Semi-automatic composition of loop transformations for deep parallelism and memory hierarchies," *IJPP*, 2006.

[6] J. Xue, *Loop Tiling for Parallelism.* Boston: Kluwer Academic Publishers, 2000.

[7] M. M. Baskaran, J. Ramanujam, and P. Sadayappan, "Automatic c-to-cuda code generation for affine programs," in *CC*, 2010.

[8] "Whirl represented as polyhedra - interface tool," http://www.lri.fr/ girbal/site_wrapit/.

[9] M. Baskaran, U. Bondhugula, S. Krishnamoorthy, J. Ramanujam, A. Rountev, and P. Sadayappan, "Automatic data movement and computation mapping for multi-level parallel architectures with explicitly managed memories," in *PPoPP*, 2008.

[10] E. Agullo, J. Demmel, J. Dongarra, N. Hadri, J. Kurzak, J. Langou, H. Ltaief, P. Luszczek, and S. Tomov, "Numerical linear algebra on emerging architectures: The plasma and magma projects," *Journal of Physics: Conference Series*, 2009.

[11] M. Frigo, "A fast fourier transform compiler," in *PLDI*, 1999.

[12] M. Puschel, J. M. F. Moura, J. Johnson, D. Padua, M. Veloso, B. Singer, J. Xiong, F. Franchetti, A. Gacic, Y. Voronenko, K. Chen, R. W. Johnson, and N. Rizzolo, "Spiral: Code generation for dsp transforms," in *Proc. IEEE, special issue on "Program Generation, Optimization, and Adaptation"*, 2005.

[13] S. Williams, L. Oliker, R. W. Vuduc, J. Shalf, and J. D. K. A. Yelick, "Optimization of sparse matrix-vector multiplication on emerging multicore platforms," in *Proc. Supercomputing*, 2007.

[14] K. Datta, M. Murphy, V. Volkov, S. Williams, J. Carter, L. Oliker, D. A. Patterson, J. Shalf, and K. A. Yelick, "Stencil computation optimization and auto-tuning on state-of-the-art multicore architectures," in *Proc. Supercomputing*, 2008.

[15] C. Chen, J. Chame, and M. W. Hall, "Combining models and guided empirical search to optimize for multiple levels of the memory hierarchy," in *CGO*, 2005.

[16] K. Yotov, X. Li, G. Ren, M. Cibulskis, G. DeJong, M. Garzaran, D. A. Padua, K. Pingali, P. Stodghill, and P.Wu, "A comparison of empirical and model-driven optimization," in *PLDI*, 2003.

[17] L. Almagor, K. Cooper, A. Grosul, T. J. Harvey, S. W. Reeves, D. Subramanian, L. Torczon, and T.Waterman, "Finding effective compilation sequences," in *LCTES*, 2004.

[18] F. Bodin, T. Kisuki, P. Knijnenburg, M. O'Boyle, and E. Rohou, "Iterative compilation in a non-linear optimisation space," in *Workshop on Profile Directed Feedback-Compilation, PACT'98*, 1998.

[19] P. Kulkarni, W. Zhao, H. Moon, K. Cho, D. Whalley, J. Davidson, M. Bailey, Y. Park, and K. Gallivan, "Finding effective optimization phase sequences," in *LCTES*, 2003.

[20] K. Cooper, P. Schielke, and D. Subramanian, "Optimizing for reduced code space using genetic algorithms," in *LCTES*, 1999.

[21] D. Barthou, S. Donadio, A. Duchateau, W. Jalby, and E. Courtois, "Iterative compilation with kernel exploration," in *LCPC*, 2007.

[22] T. Kisuki, P. M. W. Knijnenburg, M. F. P. O'Boyle, F. Bodin, and H. A. G. Wijshoff, "A feasibility study in iterative compilation," in *Proc. International Symposium on High Performance Computing*, 1999.

[23] G. Fursin, A. Cohen, M. O'Boyle, and O. Temam, "A practical method for quickly evaluating program optimizations," in *HiPEAC*, 2005.

[24] J. Cavazos and J. E. Moss, "Inducing heuristics to decide whether to schedule," in *PLDI*, 2004.

[25] F. Agakov, E. Bonilla, J. Cavazos, B. Franke, G. Fursin, M. F. P. O'Boyle, J. Thomson, M. Toussaint, , and C. K. I. Williams, "Using machine learning to focus iterative optimization," in *CGO*, 2006.

[26] Y. Liu, E. Zhang, and X. Shen, "A cross-input adaptive framework for gpu programs optimization," in *IPDPS*, 2009.

[27] G. Fursin and O. Temam, "Collective optimization," in *HiPEAC*, 2009.

[28] "Collective tuning," http://ctuning.org/cbench.

[29] G. Fursin, C. Miranda, O. Temam, M. Namolaru, E. Yom-Tov, A. Zaks, B. Mendelson, P. Barnard, E. Ashton, E. Courtois, F. Bodin, E. Bonilla, J. Thomson, H. Leather, C. Williams, and M. O'Boyle, "Milepost gcc: machine learning based research compiler," in *Proceedings of the GCC Developers' Summit*, 2008.

[30] M. Hall, J. Chame, C. Chen, J. Shin, G. Rudy, and M. Khan, "Loop transformation recipes for code generation and auto-tuning," in *LCPC*, 2009.

[31] S. Donadio, J. Brodman, T. Roeder, K. Yotov, D. Barthou, A. Cohen, M. J. Garzaran, D. Padua, and K. Pingali, "A language for the compact representation of multiple program versions," in *LCPC*, 2005.